Front. Phys. China, 2010, 5(2): 188–198
DOI 10.1007/s11467-010-0007-9

RESEARCH ARTICLE

Thermodynamic properties of a spin half ladder system

Hoi Yin SHIK (石海燕)†, **Ru CHEN** (陈茹)

Department of Physics and the Institute of Theoretical Physics, The Chinese University of Hong Kong, Hong Kong, China
E-mail: hyshik@alumni.cuhk.net

Received January 27, 2010; accepted February 1, 2010

A complete dimerized state exists for one kind of two-leg spin half ladders, which has local antiferromagnetic ordering and frustration effect at the same time. The system's low-lying excitations can be obtained exactly which enables us to calculate thermodynamic quantities such as specific heat and magnetic susceptibility at low temperatures. Our results also show that the subset energy spectrum is a good approximation to the whole spectrum even for the usual two-leg spin half ladder without frustration.

Keywords spin system, exact soluble model

PACS numbers 75.10.Jm, 75.40.Cx

1 Introduction

The Heisenberg model [1] is still widely studied as it describes magnetic properties of many materials and because of its intrinsic theoretical interest [2]. In particular, the discovery of high-temperature superconductivity in the copper oxide compounds [3, 4] and the resonating-valence-bond theory proposed by Anderson [5, 6] arouse much interest in the low-dimensional antiferromagnetic (AF) systems. Recently, much attention paid in quantum spin models focused on its entanglement [7–16] which is related to quantum information [17, 18].

Although the Heisenberg model looks simple, it has not yet been solved analytically exactly apart from one dimension [19] and at Ising limit [20] in two dimensions [21]. Great effort has been placed to solve the model using various approaches. One such approach is the construction of soluble models. An exact soluble dimerized state is found in the one-dimensional Majumdar–Ghosh model [22] and the two-dimensional model proposed by Shastry and Sutherland (SS) [23], where the ground state is a product of singlet dimers. The elementary excitation can be constructed as a pair of unbound spins above the completely dimerized state [24]. Recently, as suggested by Lin and Shen, the one-, two- or three- dimensional net spin models for general spin [25] also have complete dimerized ground state. The ground state and first excited state of these exact soluble net spin models were studied in detail [26].

Due to complexity in the energy spectrum, there exists very few studies at finite temperatures, and most of them are numerical, e.g., the well-known work of Bonner and Fisher [27]. In this work, we would like to contribute to finite temperature studies of the Heisenberg model by studying the low-lying excitations and hence the thermodynamic properties of an AF spin half ladder [28–35]. The general spin ladder can be regarded as a strip made up of two-dimensional square lattices, and its properties help us in the understanding of high-temperature superconductivity [36] as mentioned at the beginning. There exists no analytical solution for general spin ladder. Nevertheless, a K-rung net spin ladder as shown in Fig. 1 can be studied in a partial analytical exact way. The model has $2K = N$ sites, and each leg connects to other leg not only perpendicularly (J_1), but also diagonally (γJ_2), with open boundary conditions imposed. $\boldsymbol{S}$ and $\boldsymbol{S}'$ represent spins on the lower and upper legs, respectively. The model Hamiltonian is

$$H = 2J_1 \sum_{i=1}^{K} \boldsymbol{S}_i \cdot \boldsymbol{S'}_i + 2J_2 \sum_{i=1}^{K-1} [\boldsymbol{S}_i \cdot \boldsymbol{S}_{i+1} + \boldsymbol{S'}_i \cdot \boldsymbol{S'}_{i+1} + \gamma(\boldsymbol{S}_{i+1} \cdot \boldsymbol{S'}_i + \boldsymbol{S}_i \cdot \boldsymbol{S'}_{i+1})] \quad (1)$$

where $J_1, J_2 \geqslant 0$, and $\gamma = 0$ or 1.

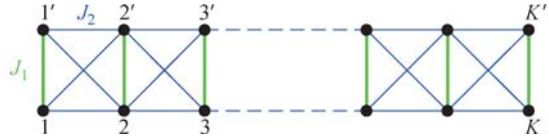

Fig. 1 The net spin ladder.

Although the model at exact soluble limit, $\gamma = 1$, has restriction in its applicability, it may give insights into some general properties of the more commonly used

model at $\gamma = 0$. Indications as shown in Fig. 2 (a) and (b) are the heat capacity and the susceptibility as function of temperature at $J_2/J_1 = 0.2$, which are very similar for both values of γ. Therefore, we investigate the model at $\gamma = 1$ to give us some ideas about its thermodynamical properties of the model at other values of γ. The difference between $\gamma = 0$ and 1 in other J_2/J_1 regime will be discussed later.

From the experimental point of view, a number of materials can be matched with the theoretical properties of two-leg Heisenberg AF ladder, such as $SrCu_2O_3$, $La_6Ca_8Cu_{24}O_{41}$ and $(VO)_2P_2O_7$ [37]. A review of certain materials well described by ladder models was proposed by Dagotto [38]. The exact soluble model ($\gamma = 1$) can be regarded as a chain of edge-sharing tetrahedra [39]. A number of materials can be matched with corner-sharing tetrahedra, such as $Tb_2Ti_2O_7$ [40] and $CsNiCrF_6$ [41]; thus, edge-sharing tetrahedra may have its experimental realization in certain compounds, just like the SS model had found its experimental realization in compound $SrCu_2(BO_3)_2$ [42–45] after it had been proposed for twenty years.

2 Low-lying excitations

We first consider the case when γ is equal to one, where the Hamiltonian can be treated analytically. The K-rung spin half ladder is equivalent to a K-site spin one chain.

The effective Hamiltonian is

$$H = -\frac{3}{2}KJ_1 + J_1\sum_{i=1}^{K}\boldsymbol{\sigma}_i^2 + 2J_2\sum_{i=1}^{K-1}\boldsymbol{\sigma}_i\cdot\boldsymbol{\sigma}_{i+1} \qquad (2)$$

where $\boldsymbol{\sigma}_i = \boldsymbol{S}_i + \boldsymbol{S'}_i$.

By inspecting the effective Hamiltonian Eq. (2), we notice that the complete dimerized state is the ground state in the limit of large J_1. The state with one broken dimer is the first excited state. So we expect that more dimers will be broken in the higher excited states. In fact, for spin half case, the ground state is the complete dimerized state when J_2/J_1 is smaller than 0.7135 [46, 47]. When J_2/J_1 is greater than 0.7135, the regime is the Haldane gap phase [48, 49]. The ground state is that of spin-1 chain with coupling $2J_2$. We take J_2/J_1 equal to 0.2 to investigate the behaviour in the large J_1 limit and take J_2/J_1 equal to 0.7 (just before the Haldane regime) to investigate the behaviour in the small J_1 limit. Besides, at J_2/J_1 equal to 0.5, the first excited state changes from a triplet to a non-dimer singlet. Hence, we take J_2/J_1 equal to 0.5 to examine the effect of level-crossing of excited states on thermodynamic properties. The excited states start crossing even when J_1 is large, but such level-crossing involves increasingly more low-lying excited states when J_1 decreases. The level crossing between the energy levels is independent of ladder size.

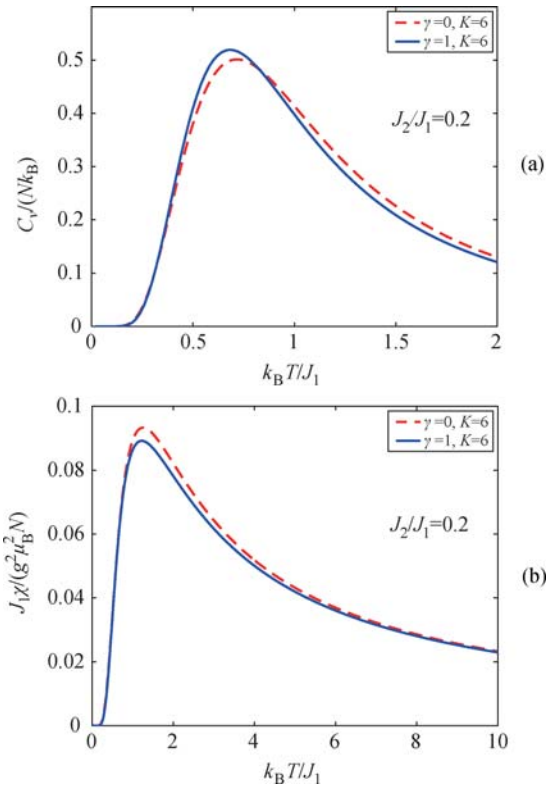

Fig. 2 **(a)** Heat capacity and **(b)** susceptibility against k_BT for $K = 6$ when $J_2/J_1 = 0.2$.

For a K-rung spin ladder with $2K$ sites, a $C_N^K \times C_N^K$ matrix is needed to be diagonalized. For $K \leqslant 3$, we can obtain all the eigenvalues analytically. However, for $K \geqslant 4$, we need to solve part of it by some exact numerical calculations. Since there is rotational symmetry in the spin space, the Hamiltonian is a function of total spin ($S_{\rm tot}$). Thus, the eigenenergies are independent of the value of z-component of total spin ($S_{\rm tot}^z$). So, we here just consider the eigenstates in zero $S_{\rm tot}^z$ subspace. Say for $K = 4$, we should consider a 70×70 matrix, but only some of the eigenvalues of the matrix have analytical form. For even larger K, say greater than 12, we cannot even use exact diagonalization (ED) to solve the Hamiltonian.

Although the whole spectrum of the infinite long spin ladder cannot be found, a partial spectrum up to certain energy scale, say $12J_1$, can be obtained. In this paper, the whole spectrum for finite size ladders up to 6 rungs, i.e. 12 sites were found. For 6-rung ladder, 238 distinct eigenlevels in the form of linear combination of J_1 and J_2 are obtained. In our approach, these eigenlevels serve as a partial spectrum for any $K \geqslant 7$. Moreover, the corresponding degeneracy of the eigenlevels in real ($D_{\rm real}$) and spin ($D_{\rm spin}$) space were found. The first 100 eigenlevels of the energy spectrum and corresponding degeneracies for any K-rung spin ladder with eigenenergies in ascending order in the large J_1 limit are listed in Tables 1–3.

Table 1 The energy spectrum from 0 to $8J_1$ for K-rung spin ladder with $E_0 = -\frac{3}{2}KJ_1$ is set to be zero.

Eigenvalue	Eigenvector	D_{real}	S_{tot}	D_{spin}	D_{total}
0	all φ_{d}	1	0	1	1
$2J_1$	$1\varphi_{\text{t}}$	K	1	3	$3K$
$4J_1-4J_2$	$\boxtimes_0$	$K-1$	0	1	$K-1$
$4J_1-2J_2$	$\boxtimes_1$	$K-1$	1	3	$3(K-1)$
$4J_1$	$2\varphi_{\text{t}}$	$\frac{1}{2!}(K-1)(K-2)$	2,1,0	9	$\frac{9}{2}(K-1)(K-2)$
$4J_1+2J_2$	$\boxtimes_2$	$K-1$	2	5	$5(K-1)$
$6J_1-6J_2$	$GS(3)$	$K-2$	1	3	$3(K-2)$
$6J_1-4J_2$	$\varphi_{\text{t}}\boxtimes_0$	$(K-2)(K-3)$	1	3	$3(K-2)(K-3)$
	$1^{\text{st}}(3)$	$K-2$	0	1	$K-2$
$6J_1-2J_2$	$\varphi_{\text{t}}\boxtimes_1$	$(K-2)(K-3)$	2,1,0	9	$9(K-2)(K-3)$
	$2^{\text{nd}}(3)$	$K-2$	2,1	8	$8(K-2)$
$6J_1$	$3\varphi_t$	$\frac{(K-2)(K-3)(K-4)}{3!}$	3,2,1/2,1,0/1	27	$\frac{9(K-2)(K-3)(K-4)}{2}$
	$3^{\text{rd}}(3)$	$K-2$	1	3	$3(K-2)$
$6J_1+2J_2$	$\varphi_{\text{t}}\boxtimes_2$	$(K-2)(K-3)$	3,2,1	15	$15(K-2)(K-3)$
	$4^{\text{th}}(3)$	$K-2$	2	5	$5(K-2)$
$6J_1+4J_2$	$5^{\text{th}}(3)$	$K-2$	3	7	$7(K-2)$
$8J_1-2J_2(4.646)$	$GS(4)$	$K-3$	0	1	$K-3$
$8J_1-2J_2(4.137)$	$1^{\text{st}}(4)$	$K-3$	1	3	$3(K-3)$
$8J_1-8J_2$	$\boxtimes_0\boxtimes_0$	$\frac{1}{2!}(K-3)(K-4)$	0	1	$\frac{1}{2}(K-3)(K-4)$
$8J_1-6J_2$	$\boxtimes_0\boxtimes_1$	$(K-3)(K-4)$	1	3	$3(K-3)(K-4)$
	φ_{t} $GS(3)$	$(K-3)(K-4)$	2,1,0	9	$9(K-3)(K-4)$
$8J_1-2J_2(2.791)$	$2^{\text{nd}}(4)$	$K-3$	2	5	$5(K-3)$
$8J_1-2J_2(2.618)$	$3^{\text{rd}}(4)$	$K-3$	1	3	$3(K-3)$
$8J_1-2J_2(2.241)$	$4^{\text{th}}(4)$	$K-3$	1	3	$3(K-3)$
$8J_1-4J_2$	$2\varphi_{\text{t}}\boxtimes_0$	$\frac{(K-3)(K-4)(K-5)}{2!}$	2,1,0	9	$\frac{9(K-3)(K-4)(K-5)}{2}$
	$\boxtimes_1\boxtimes_1$	$\frac{1}{2!}(K-3)(K-4)$	2,1,0	9	$\frac{9}{2}(K-3)(K-4)$
	φ_{t} $1^{\text{st}}(3)$	$(K-3)(K-4)$	1	3	$3(K-3)(K-4)$
	$5^{\text{th}}(4)$	$K-3$	0	1	$K-3$
$8J_1-2J_2(1.618)$	$6^{\text{th}}(4)$	$K-3$	2	5	$5(K-3)$
$8J_1-2J_2$	$2\varphi_{\text{t}}\boxtimes_1$	$\frac{(K-3)(K-4)(K-5)}{2!}$	3,2,1/2,1,0/1	27	$\frac{27(K-3)(K-4)(K-5)}{2}$
	$\boxtimes_0\boxtimes_2$	$(K-3)(K-4)$	2	5	$5(K-3)(K-4)$
	φ_{t} $2^{\text{nd}}(3)$	$(K-3)(K-4)$	3,2,1/2,1,0	24	$24(K-3)(K-4)$
	$7^{\text{th}}(4)$	$K-3$	2	5	$5(K-3)$
$8J_1-2J_2(0.759)$	$8^{\text{th}}(4)$	$K-3$	1	3	$3(K-3)$
$8J_1-2J_2(0.414)$	$9^{\text{th}}(4)$	$K-3$	3	7	$7(K-3)$
$8J_1-2J_2(0.382)$	$10^{\text{th}}(4)$	$K-3$	1	3	$3(K-3)$
$8J_1$	$4\varphi_{\text{t}}$	$\frac{(K-3)(K-4)(K-5)(K-6)}{4!}$	4,3*3,6*2,6*1,3*0	81	$\frac{27(K-3)(K-4)(K-5)(K-6)}{8}$
	$\boxtimes_1\boxtimes_2$	$(K-3)(K-4)$	3,2,1	15	$15(K-3)(K-4)$
	φ_{t} $3^{\text{rd}}(3)$	$(K-3)(K-4)$	2,1,0	9	$9(K-3)(K-4)$
	$11^{\text{th}}(4)$	$K-3$	2	5	$5(K-3)$
$8J_1+2J_2(0.618)$	$12^{\text{th}}(4)$	$K-3$	2	5	$5(K-3)$
$8J_1+2J_2(0.645)$	$13^{\text{th}}(4)$	$K-3$	0	1	$K-3$
$8J_1+2J_2$	$2\varphi_t\boxtimes_2$	$\frac{(K-3)(K-4)(K-5)}{2!}$	4,3,2,1,0/3,2,1/2	45	$\frac{45(K-3)(K-4)(K-5)}{2}$
	φ_{t} $4^{\text{th}}(3)$	$(K-3)(K-4)$	3,2,1	15	$15(K-3)(K-4)$
	$14^{\text{th}}(4)$	$K-3$	3	7	$7(K-3)$
$8J_1+2J_2(1.137)$	$15^{\text{th}}(4)$	$K-3$	1	3	$3(K-3)$
$8J_1+2J_2(1.791)$	$16^{\text{th}}(4)$	$K-3$	2	5	$5(K-3)$

(*continued*)

Eigenvalue	Eigenvector	D_{real}	S_{tot}	D_{spin}	D_{total}
$8J_1+4J_2$	$\boxtimes_2\boxtimes_2$	$\frac{1}{2!}(K-3)(K-4)$	4,3,2,1,0	25	$\frac{25}{2}(K-3)(K-4)$
	$\varphi_{\text{t}}\ 5^{\text{th}}(3)$	$(K-3)(K-4)$	4,3,2	21	$21(K-3)(K-4)$
$8J_1+2J_2(2.414)$	$17^{\text{th}}(4)$	$K-3$	3	7	$7(K-3)$
$8J_1+6J_2$	$18^{\text{th}}(4)$	$K-3$	4	9	$9(K-3)$

Table 2 The energy spectrum with $10J_1$ and negative J_2 for K-rung spin ladder with $E_0=-\frac{3}{2}KJ_1$ is set to be zero.

Eigenvalue	Eigenvector	D_{real}	S_{tot}	D_{spin}	D_{total}
$10J_1-2J_2(5.830)$	$GS(5)$	$K-4$	1	3	$3(K-4)$
$10J_1-2J_2(5.284)$	$1^{\text{st}}(5)$	$K-4$	0	1	$K-4$
$10J_1-10J_2$	$\boxtimes_0 GS(3)$	$(K-4)(K-5)$	1	3	$3(K-4)(K-5)$
$10J_1-2J_2(4.646)$	$\varphi_{\text{t}}GS(4)$	$(K-4)(K-5)$	1	3	$3(K-4)(K-5)$
$10J_1-2J_2(4.405)$	$2^{\text{nd}}(5)$	$K-4$	2	5	$5(K-4)$
$10J_1-2J_2(4.397)$	$3^{\text{rd}}(5)$	$K-4$	1	3	$3(K-4)$
$10J_1-2J_2(4.137)$	$\varphi_{\text{t}}1^{\text{st}}(4)$	$(K-4)(K-5)$	2,1,0	9	$9(K-4)(K-5)$
$10J_1-8J_2$	$\varphi_{\text{t}}\boxtimes_0\boxtimes_0$	$\frac{(K-4)(K-5)(K-6)}{2!}$	1	3	$\frac{3(K-4)(K-5)(K-6)}{2}$
	$\boxtimes_1 GS(3)$	$(K-4)(K-5)$	2,1,0	9	$9(K-4)(K-5)$
	$\boxtimes_0 1^{\text{st}}(3)$	$(K-4)(K-5)$	0	1	$(K-4)(K-5)$
	$4^{\text{th}}(5)$	$K-4$	0	1	$K-4$
$10J_1-2J_2(3.823)$	$5^{\text{th}}(5)$	$K-4$	1	3	$3(K-4)$
$10J_1-2J_2(3.473)$	$6^{\text{th}}(5)$	$K-4$	2	5	$5(K-4)$
$10J_1-2J_2(3.412)$	$7^{\text{th}}(5)$	$K-4$	1	3	$3(K-4)$
$10J_1-6J_2$	$\varphi_{\text{t}}\boxtimes_0\boxtimes_1$	$(K-4)(K-5)(K-6)$	2,1,0	9	$9(K-4)(K-5)(K-6)$
	$2\varphi_{\text{t}}GS(3)$	$\frac{(K-4)(K-5)(K-6)}{2!}$	3,2,1/2,1,0/1	27	$\frac{27(K-4)(K-5)(K-6)}{2}$
	$\boxtimes_1 1^{\text{st}}(3)$	$(K-4)(K-5)$	1	3	$3(K-4)(K-5)$
	$\boxtimes_0 2^{\text{nd}}(3)$	$(K-4)(K-5)$	2,1	8	$8(K-4)(K-5)$
$10J_1-2J_2(2.825)$	8th(5)	$K-4$	1	3	$3(K-4)$
$10J_1-2J_2(2.791)$	$\varphi_{\text{t}}2^{\text{nd}}(4)$	$(K-4)(K-5)$	3,2,1	15	$15(K-4)(K-5)$
$10J_1-2J_2(2.732)$	$9^{\text{th}}(5)$	$K-4$	2	5	$5(K-4)$
$10J_1-2J_2(2.618)$	$\varphi_{\text{t}}3^{\text{rd}}(4)$	$(K-4)(K-5)$	2,1,0	9	$9(K-4)(K-5)$
$10J_1-2J_2(2.575)$	$10^{\text{th}}(5)$	$K-4$	1	3	$3(K-4)$
$10J_1-2J_2(2.411)$	$11^{\text{th}}(5)$	$K-4$	1	3	$3(K-4)$
$10J_1-2J_2(2.375)$	$12^{\text{th}}(5)$	$K-4$	3	7	$7(K-4)$
$10J_1-2J_2(2.337)$	$13^{\text{th}}(5)$	$K-4$	0	1	$K-4$
$10J_1-2J_2(2.241)$	$\varphi_{\text{t}}4^{\text{th}}(4)$	$(K-4)(K-5)$	2,1,0	9	$9(K-4)(K-5)$
$10J_1-2J_2(2.237)$	$14^{\text{th}}(5)$	$K-4$	2	5	$5(K-4)$
$10J_1-4J_2$	$3\varphi_{\text{t}}\boxtimes_0$	$\frac{(K-4)(K-5)(K-6)(K-7)}{3!}$	3,2,1/2,1,0/1	27	$\frac{27(K-4)(K-5)(K-6)(K-7)}{6}$
	$\varphi_{\text{t}}\boxtimes_1\boxtimes_1$	$\frac{(K-4)(K-5)(K-6)}{2!}$	3,2,1/2,1,0/1	27	$\frac{27(K-4)(K-5)(K-6)}{2}$
	$2\varphi_t 1^{\text{st}}(3)$	$\frac{(K-4)(K-5)(K-6)}{2!}$	2,1,0	9	$\frac{9(K-4)(K-5)(K-6)}{2}$
	$\boxtimes_0 3^{\text{rd}}(3)$	$(K-4)(K-5)$	1	3	$3(K-4)(K-5)$
	$\boxtimes_1 2^{\text{nd}}(3)$	$(K-4)(K-5)$	3,2,1/2,1,0	24	$24(K-4)(K-5)$
	$\boxtimes_2 GS(3)$	$(K-4)(K-5)$	3,2,1	15	$15(K-4)(K-5)$
	$\varphi_{\text{t}}5^{\text{th}}(4)$	$(K-4)(K-5)$	1	3	$3(K-4)(K-5)$
	$15^{\text{th}}(5)$	$K-4$	2	5	$5(K-4)$
$10J_1-2J_2(1.818)$	$16^{\text{th}}(5)$	$K-4$	2	5	$5(K-4)$
$10J_1-2J_2(1.618)$	$\varphi_{\text{t}}6^{\text{th}}(4)$	$(K-4)(K-5)$	3,2,1	15	$15(K-4)(K-5)$
$10J_1-2J_2(1.544)$	$17^{\text{th}}(5)$	$K-4$	1	3	$3(K-4)$
$10J_1-2J_2(1.303)$	$18^{\text{th}}(5)$	$K-4$	3	7	$7(K-4)$
$10J_1-2J_2(1.184)$	$19^{\text{th}}(5)$	$K-4$	1	3	$3(K-4)$

(*continued*)

Eigenvalue	Eigenvector	$D_{\rm real}$	$S_{\rm tot}$	$D_{\rm spin}$	$D_{\rm total}$
$10J_1-2J_2$	$3\varphi_{\rm t}\boxtimes_1$	$\frac{(K-4)(K-5)(K-6)(K-7)}{3!}$	4,3*3,6*2,6*1,3*0	81	$\frac{27(K-4)(K-5)(K-6)(K-7)}{2}$
	$\varphi_{\rm t}\boxtimes_0\boxtimes_2$	$(K-4)(K-5)(K-6)$	3,2,1	15	$15(K-4)(K-5)(K-6)$
	$2\varphi_{\rm t}2^{\rm nd}(3)$	$\frac{(K-4)(K-5)(K-6)}{2!}$	4,3*3,5*2,5*1,2*0	72	$36(K-4)(K-5)(K-6)$
	$\boxtimes_0 4^{\rm th}(3)$	$(K-4)(K-5)$	2	5	$5(K-4)(K-5)$
	$\boxtimes_1 3^{\rm rd}(3)$	$(K-4)(K-5)$	2,1,0	9	$9(K-4)(K-5)$
	$\boxtimes_2 1^{\rm st}(3)$	$(K-4)(K-5)$	2	5	$5(K-4)(K-5)$
	$\varphi_{\rm t}7^{\rm th}(4)$	$(K-4)(K-5)$	3,2,1	15	$15(K-4)(K-5)$
	$20^{\rm th}(5)$	$K-4$	3	7	$7(K-4)$
$10J_1-2J_2(0.894)$	$21^{\rm st}(5)$	$K-4$	1	3	$3(K-4)$
$10J_1-2J_2(0.881)$	$22^{\rm nd}(5)$	$K-4$	3	7	$7(K-4)$
$10J_1-2J_2(0.759)$	$\varphi_{\rm t}8^{\rm th}(4)$	$(K-4)(K-5)$	2,1,0	9	$9(K-4)(K-5)$
$10J_1-2J_2(0.507)$	$23^{\rm rd}(5)$	$K-4$	2	5	$5(K-4)$
$10J_1-2J_2(0.414)$	$\varphi_{\rm t}9^{\rm th}(4)$	$(K-4)(K-5)$	4,3,2	21	$21(K-4)(K-5)$
$10J_1-2J_2(0.409)$	$24^{\rm th}(5)$	$K-4$	3	7	$7(K-4)$
$10J_1-2J_2(0.382)$	$\varphi_{\rm t}10^{\rm th}(4)$	$(K-4)(K-5)$	2,1,0	9	$9(K-4)(K-5)$
$10J_1-2J_2(0.380)$	$25^{\rm th}(5)$	$K-4$	2	5	$5(K-4)$
$10J_1-2J_2(0.372)$	$26^{\rm th}(5)$	$K-4$	2	5	$5(K-4)$
$10J_1-2J_2(0.215)$	$27^{\rm th}(5)$	$K-4$	1	3	$3(K-4)$

The ground state energy $E_0=-\frac{3}{2}KJ_1$ for different K-rung ladders is set to be zero. Those 138 eigenlevels starting from $12J_1$ are relatively high in energy in the parameter range concerned because we are mainly interested in the low-temperature behavior of the model for infinite system; they are not listed in the paper in the interest of succinctness.

Notations in Tables 1–3:

For two spins at a particular rung which form a dimer $\varphi_{\rm d}$ or triplet $\varphi_{\rm t}$,

$$\varphi_{\rm d}=|S_{\rm tot},S^z_{\rm tot}\rangle=|0,0\rangle=\frac{1}{\sqrt{2}}(|\uparrow_i\downarrow_{i'}\rangle-|\downarrow_i\uparrow_{i'}\rangle)$$

$$\varphi_{\rm t}=|S_{\rm tot},S^z_{\rm tot}\rangle=|1,0\rangle=\frac{1}{\sqrt{2}}(|\uparrow_i\downarrow_{i'}\rangle+|\downarrow_i\uparrow_{i'}\rangle)$$

For four spins at two nearest rungs which form a plaquette with $S_{\rm tot}$ equal to two $\boxtimes_2$, one $\boxtimes_1$ or zero $\boxtimes_0$,

$$\boxtimes_2=\frac{1}{\sqrt{6}}\Big(|\uparrow\downarrow\rangle+|\,\downarrow\uparrow\rangle+|\downarrow\downarrow\rangle+|\uparrow\uparrow\rangle+|\uparrow\downarrow\uparrow\downarrow\rangle+|\downarrow\uparrow\downarrow\uparrow\rangle\Big)$$

$$\boxtimes_1=\frac{1}{\sqrt{2}}\Big(|\downarrow\downarrow\rangle-|\uparrow\uparrow\rangle\Big)$$

$$\boxtimes_0=\frac{1}{\sqrt{12}}\Big(|\downarrow\downarrow\rangle+|\downarrow\uparrow\rangle+|\uparrow\downarrow\rangle+|\uparrow\uparrow\rangle-2|\uparrow\downarrow\rangle-2|\downarrow\uparrow\rangle\Big)$$

For those eigenvectors that correspond to the eigenstates of the K-site spin-1 chain, they are denoted by specified state followed by (K). For example, an eigenvector corresponds to the ground state of 3-site spin-1 chain is denoted by $GS(3)$, and the second excited state of 4-site spin-1 chain is denoted by $2^{\rm nd}(4)$.

Furthermore, the degeneracies listed in the tables are valid for any K, where K is the number of rungs of the ladder and not limited to 6. For example, there are two eigenvectors, $3\varphi_{\rm t}$ and $3^{\rm rd}(3)$, that correspond to the $6J_1$ state, but $3\varphi_{\rm t}$ gives non-zero degeneracy when $K\geqslant 5$, whereas $3^{\rm rd}(3)$ gives non-zero degeneracy when $K\geqslant 3$. Thus, for $K=4$, the $6J_1$ state has $0+3(4-2)=6$ degeneracies, and for $K=7$, the $6J_1$ state has $\frac{9}{2}(7-2)(7-3)(7-4)+3(7-2)=285$ degeneracies.

One should notice that the higher excited states consist of more triplets, but none of them are adjacent, i.e. the triplets are separated by at least one dimer. In fact, when two triplets come next to each other, they will combine with each other to form a plaquette state which has lower energy that depends on the value of J_2/J_1. Furthermore, when n triplets come next to each other, they will form an eigenstate of the n-site spin-1 chain. There is attractive interaction among the triplets.

The energy spectrum of K-rung ladder is a subset of that of the K+1-rung ladder. Apart from the common eigenstates, those new eigenstates in K+1-rung ladder are eigenstates of K+1-site spin-1 chain, as well as the linear combination of eigenstates in K-rung ladder separated by at least one dimer. Hence, solving the K-rung net spin half ladder is equivalent to solving a K-site spin one chain which requires less computing space.

The 238 eigenvalues with coefficients of J_1 less than or equal to 12 are the partial spectrum selected to be used in the approximate calculations of thermodynamic properties of K-rung ladder with $K\geqslant 7$, a straightforward choice for keeping the calculation efforts comparable to

Table 3 The energy spectrum with $10J_1$ and positive J_2 for K-rung spin ladder with $E_0 = -\frac{3}{2}KJ_1$ is set to be zero.

Eigenvalue	Eigenvector	$D_{\rm real}$	$S_{\rm tot}$	$D_{\rm spin}$	$D_{\rm total}$
$10J_1$	$5\varphi_{\rm t}$	$\frac{(K-4)(K-5)(K-6)(K-7)(K-8)}{5!}$	5,4*4,10*3,15*2, 15*1,6*0	243	$\frac{81(K-4)(K-5)(K-6)(K-7)(K-8)}{40}$
	$\varphi_{\rm t}\boxtimes_1\boxtimes_2$	$(K-4)(K-5)(K-6)$	4,3,2,1,0/3,2,1/2	45	$45(K-4)(K-5)(K-6)$
	$2\varphi_{\rm t}3^{\rm rd}(3)$	$\frac{(K-4)(K-5)(K-6)}{2!}$	3,2,1/2,1,0/1	27	$\frac{27(K-4)(K-5)(K-6)}{2}$
	$\boxtimes_0 5^{\rm th}(3)$	$(K-4)(K-5)$	3	7	$7(K-4)(K-5)$
	$\boxtimes_1 4^{\rm th}(3)$	$(K-4)(K-5)$	3,2,1	15	$15(K-4)(K-5)$
	$\boxtimes_2 2^{\rm nd}(3)$	$(K-4)(K-5)$	4,3,2,1,0/3,2,1	40	$40(K-4)(K-5)$
	$\varphi_{\rm t}11^{\rm th}(4)$	$(K-4)(K-5)$	3,2,1	15	$15(K-4)(K-5)$
	$28^{\rm th}(5)$	$K-4$	3	7	$7(K-4)$
$10J_1+2J_2(0.038)$	$29^{\rm th}(5)$	$K-4$	1	3	$3(K-4)$
$10J_1+2J_2(0.382)$	$30^{\rm th}(5)$	$K-4$	4	9	$9(K-4)$
$10J_1+2J_2(0.546)$	$31^{\rm st}(5)$	$K-4$	2	5	$5(K-4)$
$10J_1+2J_2(0.618)$	$\varphi_{\rm t}12^{\rm th}(4)$	$(K-4)(K-5)$	3,2,1	15	$15(K-4)(K-5)$
$10J_1+2J_2(0.646)$	$\varphi_{\rm t}13^{\rm th}(4)$	$(K-4)(K-5)$	1	3	$3(K-4)(K-5)$
$10J_1+2J_2(0.732)$	$32^{\rm nd}(5)$	$K-4$	2	5	$5(K-4)$
$10J_1+2J_2(0.903)$	$33^{\rm rd}(5)$	$K-4$	2	5	$5(K-4)$
$10J_1+2J_2$	$3\varphi_{\rm t}\boxtimes_2$	$\frac{(K-4)(K-5)(K-6)(K-7)}{3!}$	5,3*4,6*3,7*2,6*1,2*0	135	$\frac{45(K-4)(K-5)(K-6)(K-7)}{2}$
	$2\varphi_{\rm t}4^{\rm th}(3)$	$\frac{(K-4)(K-5)(K-6)}{2!}$	4,3,2,1,0/3,2,1/2	45	$\frac{45(K-4)(K-5)(K-6)}{2}$
	$\boxtimes_1 5^{\rm th}(3)$	$(K-4)(K-5)$	4,3,2	21	$21(K-4)(K-5)$
	$\boxtimes_2 3^{\rm rd}(3)$	$(K-4)(K-5)$	3,2,1	15	$15(K-4)(K-5)$
	$\varphi_{\rm t}14^{\rm th}(4)$	$(K-4)(K-5)$	4,3,2	21	$21(K-4)(K-5)$
	$34^{\rm th}(5)$	$K-4$	3,3	14	$14(K-4)$
$10J_1+2J_2(1.036)$	$35^{\rm th}(5)$	$K-4$	1	3	$3(K-4)$
$10J_1+2J_2(1.137)$	$\varphi_{\rm t}15^{\rm th}(4)$	$(K-4)(K-5)$	2,1,0	9	$9(K-4)(K-5)$
$10J_1+2J_2(1.382)$	$36^{\rm th}(5)$	$K-4$	4	9	$9(K-4)$
$10J_1+2J_2(1.455)$	$37^{\rm th}(5)$	$K-4$	3	7	$7(K-4)$
$10J_1+2J_2(1.620)$	$38^{\rm th}(5)$	$K-4$	0	1	$K-4$
$10J_1+2J_2(1.741)$	$39^{\rm th}(5)$	$K-4$	1	3	$3(K-4)$
$10J_1+2J_2(1.791)$	$\varphi_{\rm t}16^{\rm th}(4)$	$(K-4)(K-5)$	3,2,1	15	$15(K-4)(K-5)$
$10J_1+2J_2(1.974)$	$40^{\rm th}(5)$	$K-4$	2	5	$5(K-4)$
$10J_1+4J_2$	$\varphi_{\rm t}\boxtimes_2\boxtimes_2$	$\frac{(K-4)(K-5)(K-6)}{2!}$	5,2*4,3*3,3*2,3*1,0	75	$\frac{75(K-4)(K-5)(K-6)}{2}$
	$2\varphi_{\rm t}5^{\rm th}(3)$	$\frac{(K-4)(K-5)(K-6)}{2!}$	5,4,3,2,1/3,2,1/3	63	$\frac{63(K-4)(K-5)(K-6)}{2}$
	$\boxtimes_2 4^{\rm th}(3)$	$(K-4)(K-5)$	4,3,2,1,0	25	$25(K-4)(K-5)$
$10J_1+2J_2(2.294)$	$41^{\rm st}(5)$	$K-4$	1	3	$3(K-4)$
$10J_1+2J_2(2.303)$	$42^{\rm nd}(5)$	$K-4$	3	7	$7(K-4)$
$10J_1+2J_2(2.414)$	$\varphi_{\rm t}17^{\rm th}(4)$	$(K-4)(K-5)$	4,3,2	21	$21(K-4)(K-5)$
$10J_1+2J_2(2.618)$	$43^{\rm rd}(5)$	$K-4$	4	9	$9(K-4)$
$10J_1+2J_2(2.769)$	$44^{\rm th}(5)$	$K-4$	2	5	$5(K-4)$
$10J_1+6J_2$	$\boxtimes_2 5^{\rm th}(3)$	$(K-4)(K-5)$	5,4,3,2,1	35	$35(K-4)(K-5)$
	$\varphi_{\rm t}18^{\rm th}(4)$	$(K-4)(K-5)$	5,4,3	27	$27(K-4)(K-5)$
$10J_1+2J_2(3.209)$	$45^{\rm th}(5)$	$K-4$	3	7	$7(K-4)$
$10J_1+2J_2(3.618)$	$46^{\rm th}(5)$	$K-4$	4	9	$9(K-4)$
$10J_1+8J_2$	$47^{\rm th}(5)$	$K-4$	5	11	$11(K-4)$

full spectrum of $K=6$, as the largest coefficient of J_1 of the full spectrum of a K-rung ladder is equal to $2K$. These eigenvalues also have the advantage of relatively high degeneracy. We should point out that the order of the eigenstates changes for different J_2/J_1 values, so for the partial spectrum approximation approach we used, not all of the low-lying excitations are always included in the partial spectrum for all J_2/J_1. The first 41 excitation energies (in the same order listed in Table 1) against J_2/J_1 are shown in Fig. 3 for illustration of the level-crossing in low-lying excited states. From this figure, we can see that as J_2/J_1 increases up to around 0.7, the level crossings between excited states keep increasing (some of them are not shown as the higher excited states

are omitted in the figure). As an indication, for any K, in the approximate spectrum just up to $8J_1$, more than the first 20 low-lying levels are always included when $J_2/J_1 < 0.2$, and the first 10 are always included when $J_2/J_1 < 0.5$. In fact, if the excitation energy is fixed at $6J_1$, then for $J_2/J_1 < 0.3$, the first 12 low lying levels already give good approximation; while for $J_2/J_1 < 0.6$, we need about the first 30 low lying levels.

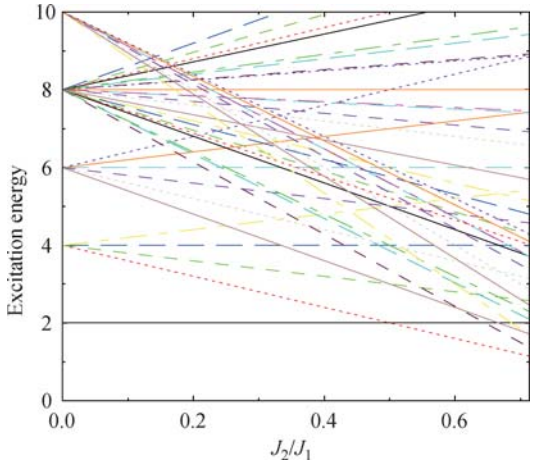

Fig. 3 The first 41 excitation energies against J_2/J_1.

The energy $\langle E\rangle$ is equal to $\dfrac{\mathrm{Tr}(\mathrm{e}^{-\beta\mathbf{H}}\mathbf{H})}{\mathrm{Tr}\,(\mathrm{e}^{-\beta\mathbf{H}})} = \dfrac{\sum_i \mathrm{e}^{-\beta E_i} E_i D_i}{\sum_i \mathrm{e}^{-\beta E_i} D_i}$, where D_i is the corresponding degeneracy of eigenenergy E_i.

The heat capacity $C_v = \dfrac{\langle E^2\rangle - \langle E\rangle^2}{kT^2}$ and the susceptibility $\chi = \dfrac{\langle m^2\rangle - \langle m\rangle^2}{kT}$ where $\langle m^2\rangle = \dfrac{\sum_i \mathrm{e}^{-\beta E_i}(S^z_{\mathrm{tot}})^2}{\sum_i \mathrm{e}^{-\beta E_i}}$ are going to be investigated.

2.1 The heat capacity

Before we extend our calculations beyond $K = 6$, the reliability of the quantities calculated by the partial spectrum is checked. The exact heat capacity calculated by the whole spectrum where leading coefficients of J_1 are up to $2K$, is compared with the approximate heat capacities estimated by three different levels of approximations: up to $2(K-1)J_1$, up to $2(K-2)J_1$, and up to $2(K-3)J_1$, as shown in Fig. 4(a)–(c). For example, for $K = 4$, the whole spectrum has eigenvalues up to $8J_1$; hence, the three approximations are $6J_1$, $4J_1$ and $2J_1$, while for $K = 6$, the whole spectrum has eigenvalues up to $12J_1$; hence, the approximations are $10J_1$, $8J_1$ and $6J_1$, respectively.

Figure 4(a)–(c) shows that the results obtained by the partial spectrum qualitatively agree with the exact one, and the approximate curves match especially well with the exact curves at lower temperature. The deviation is larger at higher temperature; the reason is because more high energy excitations, which have been omitted in the approximations, are involved at higher temperature.

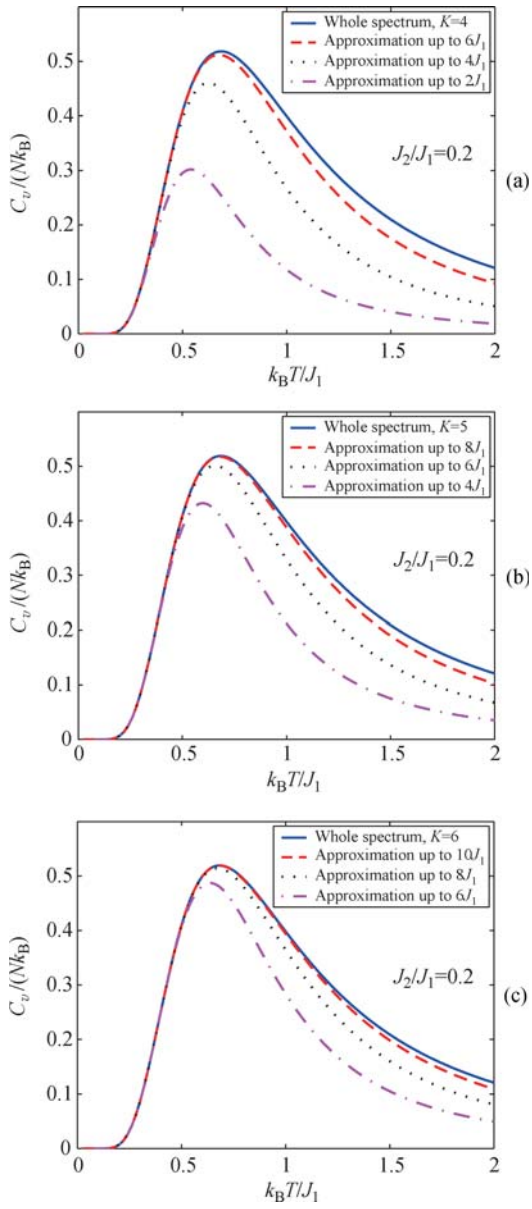

Fig. 4 Heat capacity against k_BT when $J_2/J_1 = 0.2$ for **(a)** $K = 4$, **(b)** $K = 5$ and **(c)** $K = 6$.

When we compare Fig. 4(a)–(c), we see that the deviation of the approximated curve from the exact curve is smaller for larger K since the ratio of the removed part of the whole spectrum decreases as K increases. Therefore, same-level approximation gives better results for larger K.

The deviation at the low temperature between the exact and estimated values is larger for the case $J_2/J_1 = 0.7$ (and generally, in small J_1 limit), as indicated by the fact that the deviation shown in Fig. 5 is larger than that shown in Fig. 4(c). This is because the eigenlevels with smaller coefficient of J_1 belong to the higher excited states when comparing with the states with larger coefficient of J_1 which are omitted in the approximations,

such as $E_9 = 6J_1$ is higher than $E_{17} = 8J_1 - 4J_2$ when $J_2/J_1 > 0.5$. Therefore, the deviation at lower temperature is more pronounced for larger J_2/J_1 as indicated in Fig. 5.

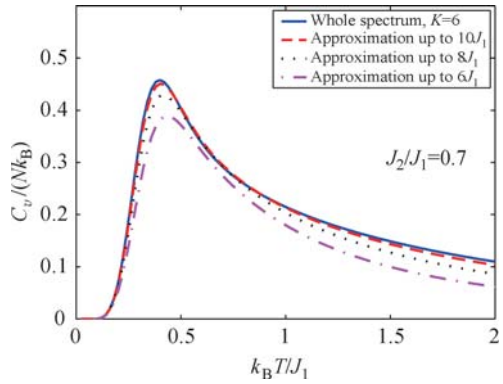

Fig. 5 Heat capacity against k_BT for $K = 6$, $J_1/J_2 = 0.7$.

Based on our numerical results, the approximations agree very well with the exact one calculated by the whole spectrum in low-temperature regime. The biggest deviation is usually around the peak value, so if the approximation is good for peak value, then it is nearly good for the whole range of temperature. Therefore, we look into the differences in peak values between the approximate and exact methods.

The peak value by the partial spectrum is always smaller than the actual value because part of the energy spectrum is always omitted in approximations. There is a systematic shift of the corresponding temperature which the heat capacity attains its maximum. The approximated curves reach the maximum at lower (higher) temperature when $J_2/J_1 = 0.2$ (0.7). The exact peak values of heat capacity C_v and the corresponding temperature k_BT for all $K = 4,\ 5,\ 6,\ 7$ (approximated) are listed in Table 4. Both of the maximum C_v and the corresponding k_BT are weak functions of the number of rungs K. Especially in the large J_1 limit, because the dimer states localize at a pair of sites only, the corresponding k_BT is nearly unchanged for $J_2/J_1 = 0.2$. However, the corresponding k_BT decreases slightly for $J_2/J_1 = 0.7$ because J_2, which makes the localized dimers couple with other sites, becomes more significant, and hence, the effect of ladder size arises. The k_BT which the C_v attains its maximum decreases as J_2/J_1 increases. This is related to the fact that the density of states in the low-energy regime increases as J_2/J_1 increases (Fig. 3).

Table 4 The peak values of heat capacity C_v and the corresponding temperature k_BT for $\gamma = 1$.

K	$J_2/J_1 = 0.2$		$J_2/J_1 = 0.5$		$J_2/J_1 = 0.7$	
	$C_v/(Nk_B)$	k_BT/J_1	$C_v/(Nk_B)$	k_BT/J_1	$C_v/(Nk_B)$	k_BT/J_1
4	0.51859	0.6835	0.53964	0.5870	0.47093	0.4555
5	0.51910	0.6835	0.54300	0.5790	0.46344	0.4225
6	0.51943	0.6835	0.54552	0.5735	0.45789	0.3990
7	0.51964	0.6820	0.54703	0.5695	0.45037	0.3855

The low-lying energy spectrum is the same for all K in large J_1 limit. Fig. 6(a) shows that the heat capacity curves are almost same for all K for large J_1 ($J_2/J_1 = 0.2$). When J_1 is small, the order of the energy levels changes. The higher energy excitations when J_1 is large become low-lying ones when J_1 is small. Hence, when J_1 is small, heat capacity curves are different for different K. In fact, the heat capacity attains a smaller maximum value at lower temperature for increasing K as shown in Fig. 6(b). In other words, the fact that the heat capacity is spectrum dependent has been illustrated in Fig. 6.

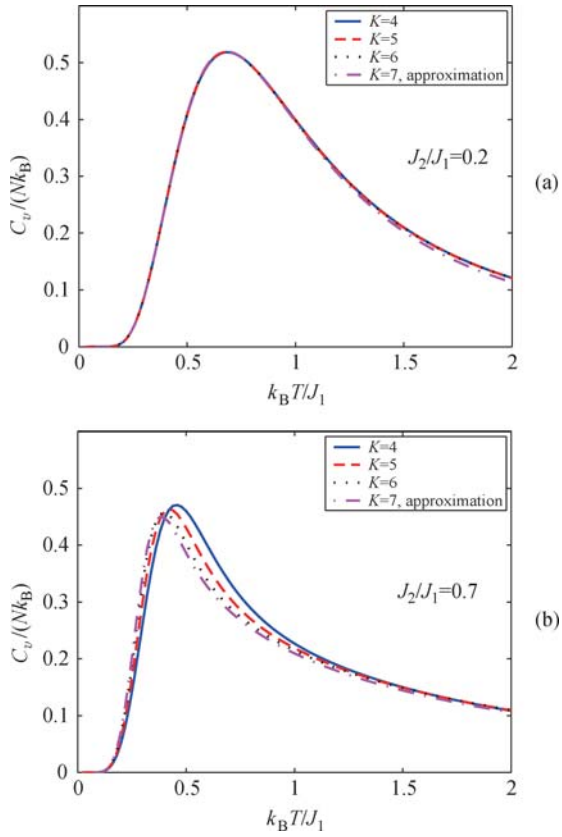

Fig. 6 Heat capacity against k_BT for J_2/J_1 equal to **(a)** 0.2 and **(b)** 0.7.

For any $K \geqslant 7$, our partial spectrum calculation gives a lower bound for the heat capacity and very good approximation at low temperature. The tendency of exact peak values of heat capacity described above indicates that the peak values for small K give an upper limit for the heat capacity for large K when $J_2/J_1 = 0.7$. Hence, the value of heat capacity for any K at low temperature can be well estimated.

2.2 The susceptibility

The properties of susceptibility are alike to those of the heat capacity due to similar reasons. To check reliability of approximation, the results for $K = 6$ when J_2/J_1 is equal to 0.7 are shown in Fig. 7. The susceptibility obtained by the partial spectrums agrees with those given

by the whole spectrum. Even when k_BT is very large, up to $10J_1$, the deviation between approximated and exact values does not increase and remains nearly unchanged once the susceptibility reaches maximum.

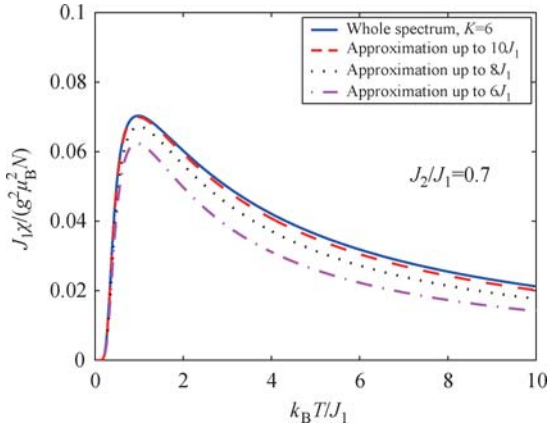

Fig. 7 Susceptibility against k_BT for $K = 6$, $J_2/J_1 = 0.7$.

In addition, the susceptibility for different K at large J_1 limit nearly coincides with each other as shown in Fig. 8(a). Even when $J_2/J_1 = 0.7$, the shift of susceptibility for different K is very small as shown in Fig. 8(b). From Table 5, the exact peak values of susceptibility χ and the corresponding temperature k_BT are nearly the same for all $K = 4$, 5, 6, 7 (approximation). The k_BT at which χ attains its maximum decreases, and also the value of maximum χ decreases, as J_2/J_1 increases.

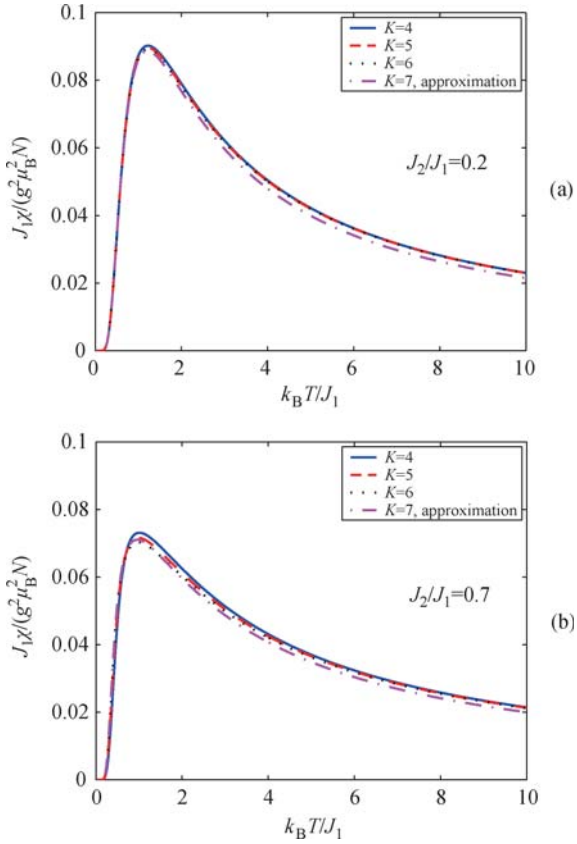

Fig. 8 Susceptibility against k_BT for J_2/J_1 equal to **(a)** 0.2 and **(b)** 0.7.

Table 5 The peak values of susceptibility χ and the corresponding temperature k_BT for $\gamma = 1$.

K	$J_2/J_1 = 0.2$		$J_2/J_1 = 0.5$		$J_2/J_1 = 0.7$	
	$\frac{J_1\chi}{g^2\mu_B^2N}$	k_BT/J_1	$\frac{J_1\chi}{g^2\mu_B^2N}$	k_BT/J_1	$\frac{J_1\chi}{g^2\mu_B^2N}$	k_BT/J_1
4	0.090246	1.2255	0.079173	1.1265	0.073125	1.0110
5	0.089616	1.2240	0.077969	1.1220	0.071613	0.9875
6	0.089197	1.2230	0.077152	1.1105	0.070319	0.9825
7	0.088694	1.2115	0.076802	1.1010	0.071051	0.9580

Similar to the heat capacity, our partial spectrum calculations give a lower bound of the susceptibility for any $K \geqslant 7$. The approximation in the sense that there is a larger range of agreement in both temperature and J_2/J_1 is better in susceptibility than in heat capacity. The tendency of exact peak values of susceptibility indicates that the peak values for small K give an upper limit for the susceptibility for large K in the whole range of J_2/J_1. Hence, the value of susceptibility for any K at low temperature can be well estimated.

2.3 For γ equal to zero

When $\gamma = 0$, the dimers formed due to antiferromagnetic coupling J_1 must be killed by the quantum fluctuation due to J_2. A dimerized state is no longer the ground state nor an eigenstate of the Hamiltonian. Moreover, the eigenlevels are not in the form of linear combinations of J_1 and J_2. In this case, the problem is solved numerically by ED. A comparison between the results of $\gamma = 0$ and 1 is made to see the difference between the soluble model and the standard Heisenberg model. Such comparison is relevant for it has been shown that the nearest-neighbor resonant-valence-bond state proposed by Anderson [5] could be a good approximation to the true ground state [50] for the 2-D antiferromagnetic Heisenberg model.

For the heat capacity, the difference between $\gamma = 0$ and 1 is less than 5% when $J_2/J_1 = 0.2$ [Fig. 2(a)]. Thus, the behaviours of these two cases are very similar in the large J_1 limit. But as J_2/J_1 increases, the quantum fluctuation due to J_2 becomes more and more important. Indeed, the energy spectrum is different for $\gamma = 0$ and 1 cases. Thus, heat capacity, which is spectrum dependent, has a large derivation between $\gamma = 0$ and 1 cases when J_2/J_1 is equal to 0.7 (Fig. 9).

For the susceptibility, the difference between $\gamma = 0$ and 1 also increases as J_2/J_1 increases. However, such difference in both the peak value and shift in k_BT is relatively small for all J_2/J_1 and K (Fig. 10). Because the susceptibility is a measure of the magnetic properties of the model, the local antiferromagnetic properties of $\gamma = 0$ should be similar to that of $\gamma = 1$. Furthermore, the difference between the values of C_v and values of χ, for $\gamma = 0$ and 1 cases is small at two temperature extremes.

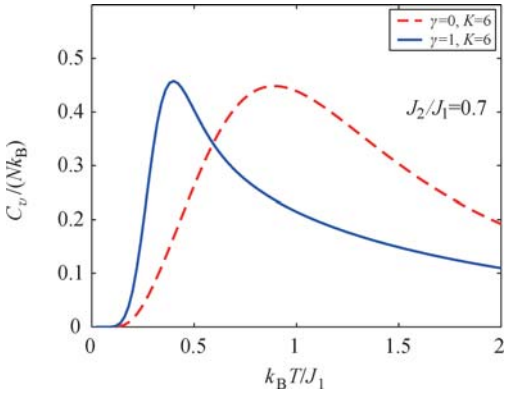

Fig. 9 C_v against k_BT for $K = 6$ when $J_2/J_1 = 0.7$.

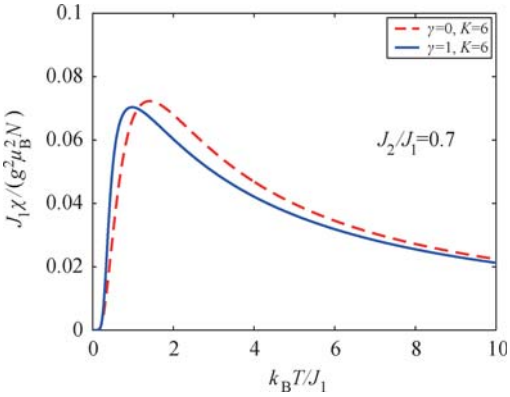

Fig. 10 χ against k_BT for $K = 6$ when $J_2/J_1 = 0.7$.

From Tables 6 and 7, the peak values of both C_v and χ decrease and the corresponding temperature increases as J_2/J_1 increases. The peak C_v when $\gamma = 1$ is greater than that when $\gamma = 0$, but the peak χ when $\gamma = 0$ is greater than that when $\gamma = 1$. Besides, in both cases, the curves reach maximum at higher temperature when $\gamma = 0$.

Table 6 The peak values of heat capacity C_v and the corresponding temperature k_BT for $\gamma = 0$.

K	$J_2/J_1 = 0.2$		$J_2/J_1 = 0.5$		$J_2/J_1 = 0.7$	
	$C_v/(Nk_B)$	k_BT/J_1	$C_v/(Nk_B)$	k_BT/J_1	$C_v/(Nk_B)$	k_BT/J_1
4	0.50256	0.7155	0.47117	0.789	0.45206	0.8735
5	0.50198	0.7165	0.46925	0.795	0.44987	0.884
6	0.50160	0.7165	0.46802	0.799	0.44859	0.891

Table 7 The peak values of susceptibility χ and the corresponding temperature k_BT for $\gamma = 0$.

K	$J_2/J_1 = 0.2$		$J_2/J_1 = 0.5$		$J_2/J_1 = 0.7$	
	$\frac{J_1\chi}{g^2\mu_B^2N}$	k_BT/J_1	$\frac{J_1\chi}{g^2\mu_B^2N}$	k_BT/J_1	$\frac{J_1\chi}{g^2\mu_B^2N}$	k_BT/J_1
4	0.093989	1.255	0.082429	1.320	0.074388	1.3995
5	0.093574	1.2555	0.081428	1.3205	0.073107	1.4085
6	0.093298	1.256	0.08076	1.324	0.07225	1.4155

3 Conclusion

By introducing the next nearest neighbour couplings γJ_2, the eigenlevels of the spin ladder can be expressed in the form of linear combinations of J_1 and J_2. Partial spectrum, 238 distinct eigenlevels, for any K with corresponding degeneracies in terms of K, where K is the number of rungs of the ladder, are obtained analytically. The partial spectrum can be regarded as an approximation to calculate heat capacity and susceptibility for any K. The validity of our approaches is verified by comparison with calculations using the whole spectrum for small-size lattice. The size dependence of these thermodynamic quantities is shown and can help to obtain the results at the thermodynamical limit.

For infinite system, the zero temperature properties of the usual spin ladder ($\gamma = 0$) can be studied by ED or DMRG, but these approaches are not applicable to the finite-temperature case. In this paper, although the obtained spectrum is for a special model ($\gamma = 1$), it is also a good approximation for the more realistic case ($\gamma = 0$). Using our approach, we found that the main features of the physical properties of the exact soluble model ($\gamma = 1$) and the usual model ($\gamma = 0$) are very similar. From the data, the shape of graphs for heat capacity and susceptibility for the two models are all alike in all cases. In particular, at low temperature or in small J_2/J_1 regime, the difference in the graphs of the two models is nearly negligible. The relatively small difference in the susceptibility shows that it is a good way to study the magnetic properties of the usual model via the exact soluble model.

Acknowledgements This work was supported in part by the Earmarked Grant for Research from the Research Grants Council (RGC) of the HKSAR, Project CUHK 401806.

References

1. W. Heisenberg, Z. Physik, 1928, 49: 619
2. H. T. Dicp, Frustrated Spin Systems, Singapore: World Scientific, 2004
3. J. G. Bednorz and K. A. Müller, Z. Phys. B, 1986, 64: 189
4. C. W. Chu, P. H. Hor, R. L. Meng, L. Gao, Z. J. Huang, and Y. Q. Wang, Phys. Rev. Lett., 1987, 58: 405
5. P. W. Anderson, Science, 1987, 235: 1196
6. P. W. Anderson, G. Baskaran, Z. Zou, and T. Hsu, Phys. Rev. Lett., 1987, 58: 2790
7. K. M. O'Connor and W. K. Wootters, Phys. Rev. A, 2001, 63: 052302
8. P. Zanardi, Phys. Rev. A, 2002, 65: 042101
9. L. F. Santos, Phys. Rev. A, 2003, 67: 062306
10. X. Wang, Phys. Lett. A, 2001, 281: 101
11. X. Wang and P. Zanardi, Phys. Lett. A, 2002, 301: 1
12. Y. Sun, Y. Chen, and H. Chen, Phys. Rev. A, 2003, 68: 044301
13. S. J. Gu, H. Q. Lin, and Y. Q. Li, Phys. Rev. A, 2003, 68: 042330
14. S. J. Gu, H. B. Li, Y. Q. Li, and H. Q. Lin, Phys. Rev. A,

2004, 70: 052302
15. S. J. Gu, G. S. Tian, and H. Q. Lin, Phys. Rev. A, 2005, 71: 052322
16. S. J. Gu, G. S. Tian, and H. Q. Lin, New J. Phys., 2006, 8: 61
17. M. A. Nilesen and I. L. Chuang, Quantum Computation and Quantum Information, Cambridge: Cambridge University Press, 2000
18. C. H. Bennett and D. P. Divincenzo, Nature, 2000, 404: 247
19. H. Bethe, Z. Physik, 1931, 71: 205
20. E. Ising, Z. Physik, 1925, 3: 253
21. L. Onsager, Phys. Rev., 1944, 65: 117
22. C. K. Majumdar and D. K. Ghosh, Math. Phys., 1969, 10: 1388
23. B. S. Shastry and B. Sutherland, Physica B, 1981, 108: 1069
24. B. S. Shastry and B. Sutherland, Phys. Rev. Lett., 1981, 47: 964
25. H. Q. Lin and J. L. Shen, J. Phys. Soc. Jpn., 2000, 69: 878
26. H. Q. Lin, J. L. Shen, and H. Y. Shik, Phys. Rev. B, 2002, 66: 184402
27. J. C. Bonner and M. E. Fisher, Phys. Rev. A, 1964, 135: 640
28. I. Bose and S. Gayen, Phys. Rev. B, 1993, 48: 10653
29. I. Bose and P. Mitra, Phys. Rev. B, 1991, 44: 443
30. Y. Xian, Phys. Rev. B, 1995, 52: 12485
31. G. Su, Phys. Lett. A, 1996, 213: 93
32. H. Niggemann, G. Uimin, and J. Zittartz, J. Phys.: Condens. Matter, 1997, 9: 9031
33. W. H. Zheng, V. Kotov, and J. Oitmaa, Phys. Rev. B, 1998, 57: 11439
34. S. Albeverio and S. M. Fei, Europhys. Lett., 1998, 41: 665
35. X. Q. Wang, Mod. Phys. Lett. B, 2000, 14: 327
36. D. J. Scalapino, Nature, 1995, 377: 12
37. E. Dagotto and T. M. Rice, Science, 1996, 271: 618
38. E. Dagotto, Rep. Prog. Phys., 1999, 62: 1525
39. M. P. Gelfand, Phys. Rev. B, 1991, 43: 8644
40. J. S. Gardner, S. R. Dunsiger, B. D. Gaulin, M. J. P. Gingras, J. E. Greedan, R. F. Kiefl, M. D. Lumsden, W. A. MacFarlane, N. P. Raju, J. E. Sonier, I. Swainson, and Z. Tun, Phys. Rev. Lett., 1999, 82: 1012
41. M. J. Harris, M. P. Zinkin, Z. Tun, B. M. Wanklyn, and I. P. Swainson, Phys. Rev. Lett., 1994, 73: 189
42. H. Kageyama, K. Yoshimura, R. Stern, N. V. Mushnikov, K. Onizuka, M. Kato, K. Kosuge, C. P. Slichter, T. Goto, and Y. Ueda, Phys. Rev. Lett., 1999, 82: 3168
43. H. Kageyama, M. Nishi, N. Aso, K. Onizuka, T. Yosihama, K. Nukui, K. Kodama, K. Kakurai, and Y. Ueda, Phys. Rev. Lett., 2000, 84: 5876
44. S. Miyahara and K. Ueda, Phys. Rev. Lett., 1999, 82: 3701
45. M. Azuma, Z. Hiroi, M. Takano, K. Ishida, and Y. Kitaoka, Phys. Rev. Lett., 1994, 73: 3463
46. S. R. White and I. Affleck, Phys. Rev. B, 1996, 54: 9862
47. H. Q. Lin, Phys. Rev. B, 1991, 44: 7151
48. F. D. M. Haldane, Phys. Lett. 1983, 93A: 464
49. F. D. M. Haldane, Phys. Rev. Lett., 1983, 50: 1153
50. S. Y. Tang and H. Q. Lin, Phys. Rev. B, 1988, 38: 6863